Environmental Science and Pollution Research (2022) 29:44504–44512
https://doi.org/10.1007/s11356-022-18949-x

RESEARCH ARTICLE

Degradation of ofloxacin by potassium ferrate: kinetics and degradation pathways

Yanghan Chen[1] · Qiuye Jin[2] · Zhaomin Tang[1]

Received: 2 August 2021 / Accepted: 25 January 2022 / Published online: 8 February 2022

Abstract

Drug residues, including various antibiotics, are being increasingly detected in aqueous environments. Ofloxacin (OFX) is one such antibiotic that is widely used in the treatment of several bacterial infections; however, chronic exposure to this antibiotic can have adverse impacts on human health. Hence, the identification of an effective OFX degradation method is essential. Thus, in this study, the degradation performance of OFX using potassium ferrate (Fe(VI)) under the influence of different initial concentrations, pH, temperature, and common ions in water was investigated. OFX degradation by Fe(VI) was directly proportional to the concentration of Fe(VI) and temperature and inversely proportional to the pH. Among the common ions in water, Fe^{3+} and NH_4^+ could significantly promote the degradation of OFX by Fe(IV), while humic acid (HA) significantly inhibited it. Under the conditions of [Fe(VI)]:[OFX] = 15:1, T = 25℃, and pH = 7.0, the removal efficiency of 8 μM OFX reached more than 90% in 4 min. Seven intermediates were identified by quadrupole time-of-flight tandem ultra-performance liquid chromatography mass spectrometry (Q-TOF LC/MS), and two possible pathways for the degradation of OFX by Fe(VI) were proposed. Overall, the results suggest that advanced oxidation technology using Fe(VI) is effective for treating wastewater containing OFX.

Keywords Ofloxacin · Advanced oxidation · Ferrate · Kinetics · Degradation pathway

Introduction

With the increasing awareness of people's environmental protection and increasing attention to health, drug residues in the environment have received increasing attention from researchers as well as the public. With the increasing use of antibiotics, high antibiotic concentrations have been detected in wastewater, as well as on the surface waters, drinking water, soil, and other environments now (Huang et al. 2019; Sanganyado and Gwenzi 2019; Cerqueira et al. 2019; Tong et al. 2019). In addition to ecotoxicity, they may cause increased bacterial resistance (Zhang et al. 2015; Hu et al. 2007). It has been reported that the proportion of drug-resistant bacteria in various poultry and livestock has also increased greatly in recent years (Van Boeckel et al. 2019).

Fluoroquinolones (FQs) have been widely used to treat a broad spectrum of bacterial infections over the past few decades (Zhang et al. 2015; Liu et al. 2016; Zhao et al. 2016). Ofloxacin (OFX), a popular FQ antibiotic, is a third-generation quinolone, which is mainly used in the treatment of acute and chronic infections of the respiratory tract, throat, and tonsils caused by gram-negative bacteria (Watanabe et al. 2001). OFX is discharged in non-metabolic form mainly through wastewater produced by the industries such as pharmaceuticals and waste generated by humans and livestock, enter into municipal wastewater treatment plants through sewer networks, and finally enter into the natural environment (Zhang et al. 2015; Jara et al. 2020; Radjenovic et al. 2007). However, existing sewage treatment facilities have low processing efficiency with regard to antibiotics (Jia et al. 2012). According to reports, various antibiotic residues have been detected in sewage treatment plants around the world, such as the average content of OFX in the effluent of sewage treatment plants has reached an astonishing

Responsible Editor: Sami Rtimi

✉ Zhaomin Tang
tl8687@163.com

[1] School of New Energy and Materials, Southwest Petroleum University, Chengdu 610500, China

[2] Faculty of Geosciences and Environmental Engineering, Southwest Jiaotong University, Sichuan 610000, China

97.0 ng/L (Wang et al. 2020a). Hence, finding an effective antibiotics degradation method is essential.

Various technologies have been developed for the removal of various antibiotics from the water now, such as adsorption, advanced oxidation processes (AOPs), biodegradation/photodegradation/sonic degradation, and membrane separation (Peng et al. 2012; Jiang et al. 2016; Gorito et al. 2018; Elmolla and Chaudhuri 2010; Wang and Wang 2019a; 2018a). However, they have not been widely applied due to their low removal efficiency and high operational cost. By contrast, advanced oxidation technology mainly generates highly active oxidation species through a series of chemical oxidation processes for the degradation of antibiotics or converts them to small molecule substances, which could enhance their biodegradability and the removal rate (Zhou et al. 2021; Sharma et al. 2016; Wilde et al. 2013; Wang and Wang 2019b; 2018b). AOPs use strong oxidation agents to degrade organic pollutants. According to the different ways used to produce oxidation agents, AOPs can be classified into many different types (Wang and Zhuan 2020; Wang and Chen 2020). Among them, Fe(VI) advanced oxidation is a promising technology for the degradation of organic pollutants in wastewater (Pi et al. 2021; Shin et al. 2018; Wang et al. 2020 b). It is characterized by rapid degradation of pollutants and high pollutant removal efficiency; hence, it can be regarded as green technology and has been widely used in wastewater treatment (Gong et al. 2020; Li et al. 2005).

In this work, K_2FeO_4 (Fe(VI)) was selected as the oxidant and OFX was selected as the target contaminant. The degradation efficiency and kinetics of OFX by Fe(VI) under different reaction conditions were investigated. In addition, on the basis of the intermediate products identified, a possible degradation pathway of OFX by Fe(VI) was proposed. This research provides theoretical support for the treatment of OFX-containing wastewater using an Fe(VI) advanced oxidation process.

Materials and methods

Reagents

All standards of the pharmaceuticals used (sodium hydroxide (NaOH), hydrochloric acid (HCl), sodium thiosulfate ($Na_2S_2O_3$), ammonium acetate (CH_3COONH_4), phosphoric acid (H_3PO_4), tert-butanol (TBA), isopropanol (IPA), sodium bicarbonate ($NaHCO_3$), sodium nitrate ($NaNO_3$), sodium sulfate (Na_2SO_4), sodium chloride (NaCl), ammonium chloride (NH_4Cl), ferric chloride ($FeCl_3$), potassium chloride (KCl), and humic acid (HA)) were of analytical purity grade and purchased from Sinopharm Chemical Reagents (Shanghai, China). The solvent (methanol) was HPLC grade and was purchased from Merck (Darmstadt, Germany). OFX was obtained from Aladdin (Shanghai, China). The water was produced using a UPH purification system (ULUP-I, Ulpure, China, resistivity ≥ 18.2 MΩcm).

Experimental procedures

Fe(VI) was prepared using a hypochlorite oxidation method (Li et al. 2005). The reaction was carried out in a 250 mL glass conical flask under a constant stirring rate of 400 rpm at 25℃ in a water bath using a thermostatic magnetic stirrer. The reaction between OFX (8.0 μM) and Fe(VI) (40.0–160.0 μM) was initiated by mixing them in equal volumes of 100.0 mL; the pH of the reaction mixtures was adjusted using 1.0 mM HCl or NaOH buffer. The reaction was quenched completely at certain reaction times (i.e., 0–5 min) using 200.0 μL of 1.0 mM $Na_2S_2O_3$ solution. Samples were filtered using 0.45 μm polytetrafluoroethylene syringe filters (Fisherbrand, Fisher Scientific) and transferred into 2.0 mL high-performance liquid chromatography (HPLC) vials for analysis. All experiments took an average of three parallel samples.

Analytical methods

The concentrations of OFX in the samples were measured by HPLC (LC-2030PLUS, Shimadzu, Japan) equipped with a SinChrom ODS-B column (5 μm, 4.6 mm × 250 mm), and the detection was performed using a G1365MWD UV detector at 293 nm. The mobile phase was composed of 60% ammonium acetate (1% phosphoric acid adjusted to pH 2.7) and 40% methanol. Samples were analyzed at a flow rate of 1.0 mL/min, the injection volume was set to 20 μL, and the column temperature was set at 25℃.

The intermediates of OFX were measured using a quadrupole time-of-flight (Q-TOF) liquid chromatography/mass spectrometry (LC/MS) (6545Q-TOF, Agilent, USA). Isocratic elution was performed at a flow rate of 0.3 mL/min with 0.1% (v/v) ammonium acetate (A) and methanol (B). The mass spectra with electrospray ionization (ESI) source were recorded across the range of 50–500 m/z in positive scan mode.

Results and discussion

Influence of initial oxidant concentration and degradation kinetics

The effect of the initial Fe(VI) concentration on OFX degradation is shown in Fig. 1a. It can be observed that the pseudo-first-order rate constants for OFX degradation (K_{obs}) increased from 0.0031 to 0.0125 s^{-1} when the Fe(VI) concentration increased from 40 to 160 μM. Then, $Ln[Fe(VI)]_0$

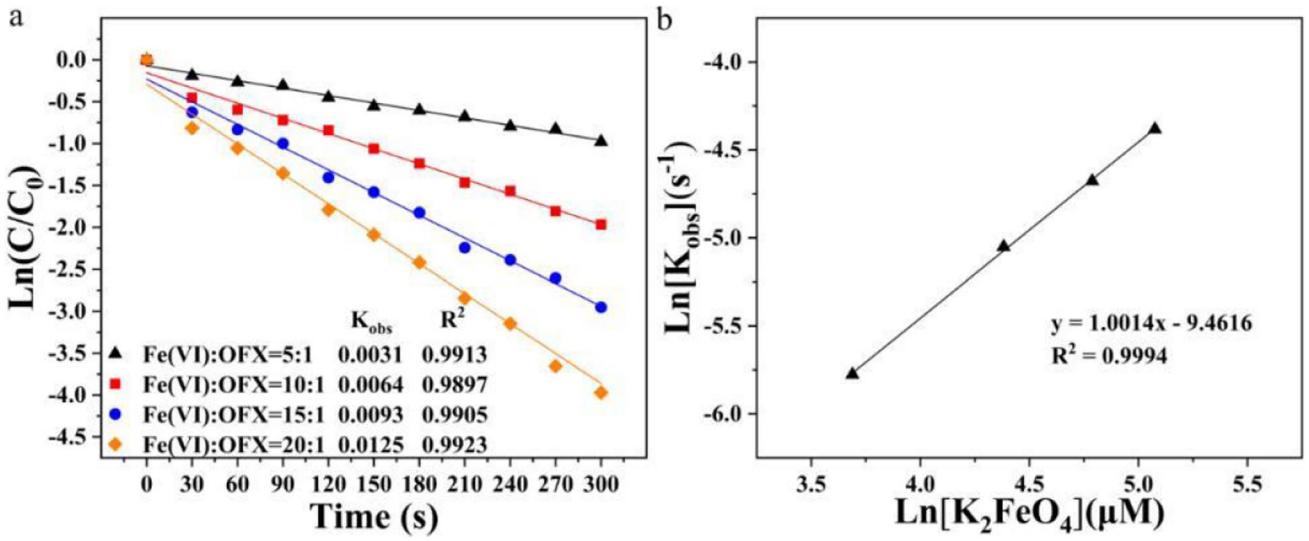

Fig. 1 Changes in OFX as a function of initial Fe(VI) concentrations. (**a**) Degradation of OFX under different initial concentrations of Fe(VI). (**b**) Linear fitting of Ln[Fe(VI)]$_0$ and LnK_{obs} at different Fe(VI) concentrations. Reaction conditions: [OFX]$_0$ = 8 μM, [Fe(VI)]$_0$ = 40–160 μM, T = 25℃, pH = 7.0

and LnK_{obs} were fitted by linear regression, and the results are shown in Fig. 1b. The correlation coefficient R^2 was greater than 0.99, which means that the degradation of OFX by Fe(VI) follows the second-order reaction kinetics equation. The rate equations under different initial concentrations of Fe(VI) are shown in Table 1.

As shown in Table 1, the average value of the secondary reaction rate constant (K_{app}) for the degradation of OFX by Fe(VI) was 78.28 M^{-1} s^{-1}. As the initial concentration of Fe(VI) increased from 40 to 160 μM, the half-life $t_{1/2}$ decreased from 224 to 55 s. The results showed that with an increase in the initial concentration of [Fe(VI)], the degradation rate of OFX gradually increased; similar results have been reported by Wang et al. (2019) and Liu et al. (2019).

Influence of pH and the corresponding kinetics

The degradation of OFX by Fe(VI) under different pH conditions was measured, and the results are shown in Fig. 2a. When the pH increased from 5 to 10, the K_{obs} decreased from 0.0168 to 0.0039 s, implying that the degradation rate of OFX by Fe(VI) increased with a decrease in the pH value; similar results have been reported by Zheng et al. (2020) and Han et al. (2018).

Because OFX and Fe(VI) have various ionisable groups, their final ionization morphologies can be determined based on different pH values (Huang et al. 2017; Peterson et al. 2015). Therefore, the kinetic equations of the pH and K_{app} values were simulated using Eq. (1)

$$K_{app}[Fe(VI)][OFX] = \sum_{i=1,2,3,j=1,2} K_{ij}a_i\beta_j[Fe(VI)][OFX] \quad (1)$$

where α_i and β_j represent the distribution coefficients of OFX and Fe(VI), respectively. When the OFX dissociation constants pK_{a1} and pK_{a2} are 6.11 and 8.18, respectively, α_1, α_2, and α_3 refer to the fractions of OFX^+, OFX^0, and OFX^-, respectively (Peterson et al. 2015). For Fe(VI) (pK_a = 7.23, pH ≥ 5 in the experiment), β_1 and β_2 refer to the fractions of $HFeO_4^-$ and FeO_4^{2-}, respectively (Han et al. 2018; Zajicek et al. 2015). Under alkaline conditions, the reaction between FeO_4^{2-} and OFX^- was very slow (Zheng et al. 2020; Han et al. 2018; Huang et al. 2017); therefore, the reaction could be ignored in the model calculation. In addition, because it was difficult for $HFeO_4^-$ and OFX^- (or FeO_4^{2-} and OFX^+)

Table 1 Kinetic equation of the degradation of OFX by Fe(VI)

[Fe(VI)]$_0$ (μM)	Kinetic equation	$t_{1/2}$ (s)	R^2	K_{app} (M^{-1} s^{-1})
40	Ln([OFX]/[OFX]$_0$) = −0.0031t–0.0541	224	0.9913	77.5
80	Ln([OFX]/[OFX]$_0$) = −0.0064t–0.1248	108	0.9897	80.0
120	Ln([OFX]/[OFX]$_0$) = −0.0093t–0.1978	75	0.9905	77.5
160	Ln([OFX]/[OFX]$_0$) = −0.0125t–0.2352	55	0.9898	78.1

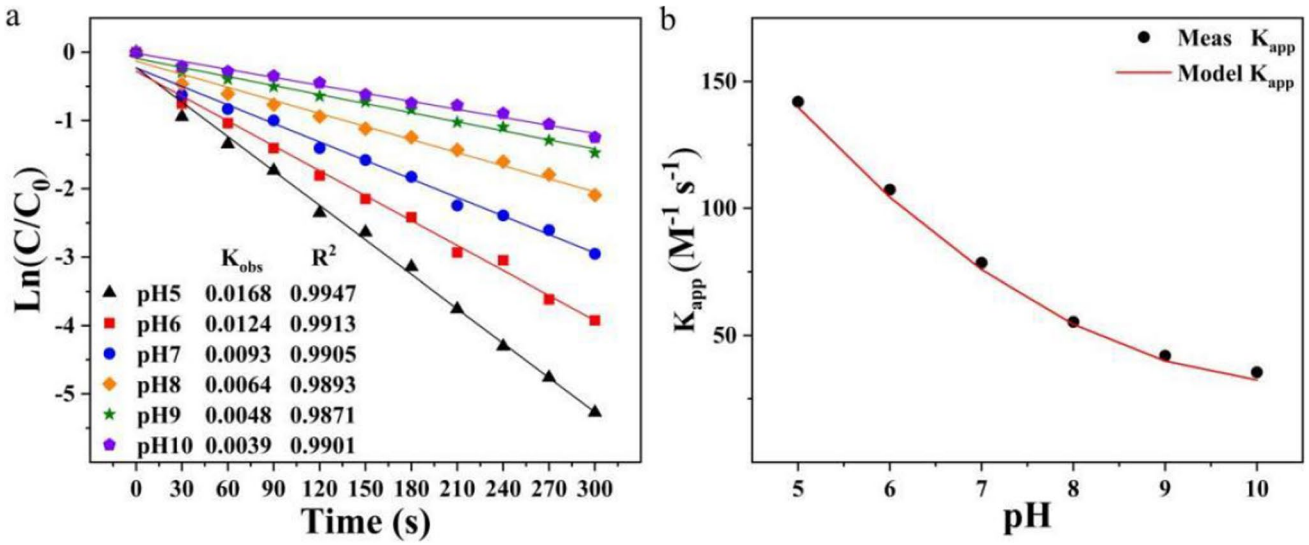

Fig. 2 Changes in OFX as a function of pH. (**a**) Degradation of OFX at different pH. (**b**) Relationship between pH value and apparent second-order reaction kinetic constant (K_{app}). Reaction conditions: $[OFX]_0 = 8$ μM, $[Fe(VI)]_0 = 120$ μM, $T = 25$℃, pH = 5–10

to exist at the same time under certain pH conditions, their reaction could also be ignored in the model calculation; therefore, the effect of pH on the K_{app} value of Fe(VI) can be further simplified as Eq. (2):

$$K_{app} = K_{11}a_1\beta_1 + K_{21}a_2\beta_1 + K_{22}a_2\beta_2 \quad (2)$$

The experimental values of K_{app} (Meas K_{app}) under different pH conditions were fitted with Eq. (2), and the results are shown in Fig. 2b; it can be seen that they exhibited a significant curve correlation ($R^2 \geq 0.99$).

The results showed that K_{11}, K_{21}, and K_{22} were 150.23 $M^{-1}S^{-1}$, 94.7 $M^{-1}S^{-1}$, and 45.1 $M^{-1}S^{-1}$, respectively. Among them, K_{11} or K_{21} was $> K_{22}$, indicating that $HFeO_4^-$ was more oxidizing than FeO_4^{2-}, and with the gradual decrease in pH (when PH ≥ 5), $HFeO_4^-$ would become more dominant in the system. Moreover, $K_{11} > K_{21}$ or K_{22} implied that $HFeO_4^-$ showed higher reactivity toward OFX^+ than OFX^0 or OFX^-. In conclusion, the degradation rate of OFX gradually increased with a continuous decrease in pH.

Influence of temperature and the corresponding kinetics

The degradation of OFX was measured as the temperature increased from 10 to 30℃; K_{obs} correspondingly increased from 0.0055 to 0.0110 s (Fig. 3a). This illustrates that the degradation rate of OFX gradually increases with an increase in temperature (Han et al. 2018). Figure 3b shows the results of fitting $\mathrm{Ln}K_{app}$ and $1000/T$, and a good linear relationship ($R^2 \geq 0.99$) can be observed. This shows that the degradation of OFX with temperature change satisfies the Arrhenius equation as follows (Luo et al. 2015; Han et al. 2018):

$$LnK_{app} = -(Ea/R) \times (1/T) + LnA \quad (3)$$

Here, the molar gas constant R is 8.314 $J \cdot mol^{-1} \cdot k^{-1}$, and hence, the reaction activation energy Ea can be calculated to be 24.2 $kJ \cdot mol^{-1}$. The results suggest that the reaction between Fe(VI) and OFX could occur even when the activation energy was relatively low.

In Fig. 3c, the results of fitting $\mathrm{Ln}(K_{app}/T)$ and $1/T$ are shown; a good linear relationship ($R^2 \geq 0.99$) is observed. This implies that the degradation of OFX with temperature change satisfies the Eying equation as follows (Luo et al. 2015):

$$\mathrm{Ln}\left(K_{app}/T\right) = -(\Delta H/R) \times (1/T) + Ln\left(K_B/h\right) + \Delta S/R \quad (4)$$

where the Boltzmann constant k_B is 1.38×10^{-23} $J \cdot k^{-1}$ and the Planck constant h is 6.626×10^{-34} $J \cdot s$; therefore, ΔH and ΔS can be calculated as 21.319 $kJ \cdot mol^{-1}$ and − 135.62 $J \cdot mol^{-1} \cdot k^{-1}$, respectively. The results show that the degradation of OFX by Fe(VI) was an endothermic reaction. With an increase in temperature, the number of effective collisions between the polymers increased, resulting in an acceleration of the reaction rate.

Influence of free radicals in reaction system

Studies have shown that the degradation of organic pollutants by Fe(VI) includes the direct oxidation by Fe(VI) and the indirect oxidation by generated free radicals (Zhang

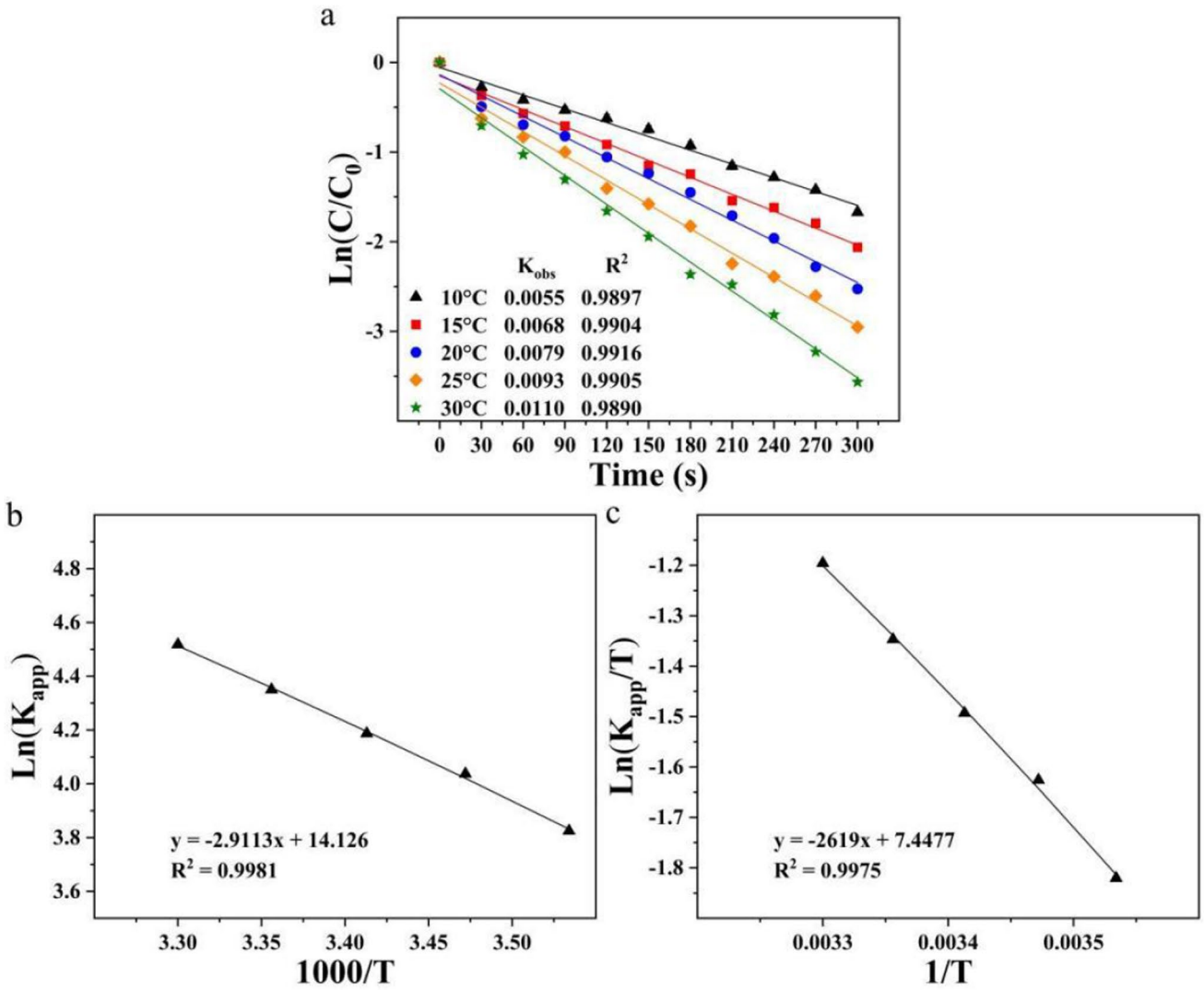

Fig. 3 Changes in OFX as a function of temperature. (**a**) Degradation of OFX at different temperatures. (**b**) Linear fitting of LnK_{app} and 1000/T. (**c**) Linear fitting of Ln(K_{app}/T) and 1/T. Reaction conditions: $[OFX]_0 = 8$ μM, $[Fe(VI)]_0 = 120$ μM, pH = 7.0; $T = 10–30$°C

et al. 2012). And Fe(VI) and its intermediates (Fe(V) and Fe(IV)) can generate highly reactive hydroxyl radicals (OH•) during their self-decomposition process (Zhang et al. 2012; Noorhasan et al. 2010). In traditional advanced oxidation process experiments, OH• plays a significant role (Wang et al. 2018; Chen et al. 2020, 2019; Wang and Wang 2020). Therefore, in order to verify the contribution of ROS, TBA and IPA were used as free radical scavengers of OH•. As shown in Fig. 4, the OFX degradation rate decreased by 4.57% and 5.82% with the addition of TBA and IPA to the reaction system, respectively. Thus, it can be concluded that Fe(VI) does exist OH• in the experiments of degrading OFX, and OH• contributed little to the degradation of OFX. Therefore, it can be considered that the degradation of OFX is mainly due to the oxidation by high-valent iron-based. Similar results have been reported by Shao et al. (2019) and Jin et al. (2021).

Influence of anions, cations, and organic matter

The common anions, cations, and organics in water were selected to investigate their influence on the degradation of OFX by Fe(IV). K^+, Na^+, Cl^-, SO_4^{2-}, and NO_3^- had almost no effect; Fe^{3+} and NH_4^+ greatly promoted OFX degradation; while HCO_3^- only had a small inhibitory effect on OFX degradation in the reaction system (Fig. 5). In addition, organic matter, represented by HA, significantly inhibited the degradation of OFX by Fe(IV) (Fig. 5).

In water, HCO_3^- can slightly inhibit the degradation of OFX by Fe(VI). On the one hand, the presence of

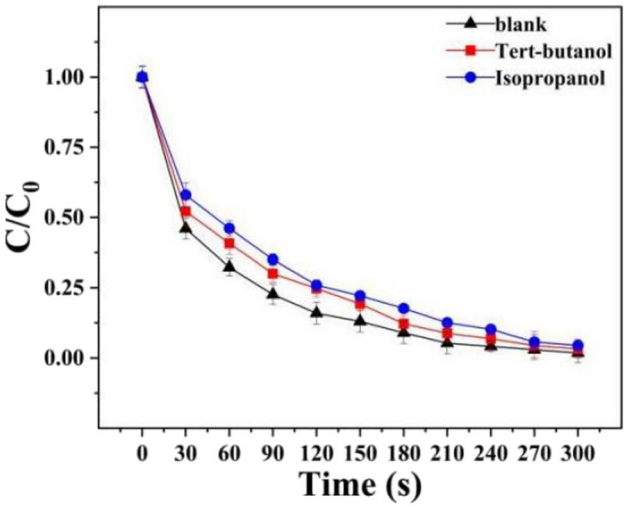

Fig. 4 Influence of $OH^•$ on OFX degradation. Reaction conditions: $[OFX]_0 = 8$ μM, $[Fe(VI)]_0 = 120$ μM, $T = 25$℃, pH = 7.0

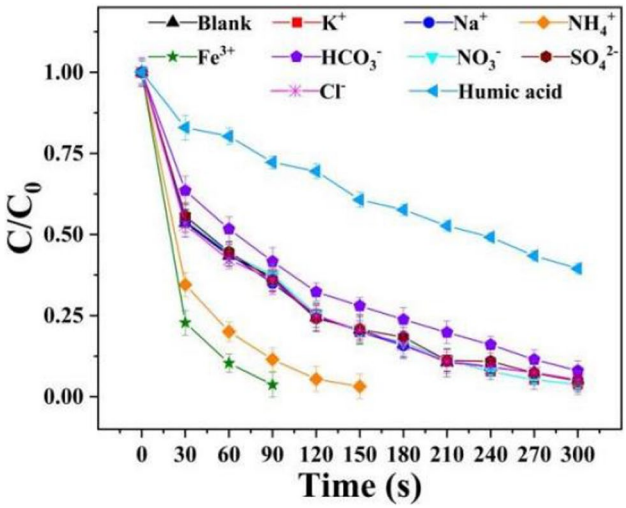

Fig. 5 OFX degradation as a function of water components. Reaction conditions: $[OFX]_0 = 8$ μM, $[Fe(IV)]_0 = 120$ μM, $[K^+]_0 = [Na^+]_0 = [NH_4^+]_0 = [Fe^{3+}]_0 = [HCO_3^-]_0 = [NO_3^-]_0 = [SO_4^{2-}]_0 = [Cl^-]_0 =$ [humic acid (HA)]$_0 = 50$ μM, $T = 25$℃, pH = 7.0

bicarbonate can increase the solution pH, which in turn affects the stability of the oxidant. As shown in Fig. 2, the degradation rate of OFX by Fe(VI) decreases with increasing pH. The reason is that Fe(VI) is more present in the form of FeO_4^{2-} under alkaline conditions, and the reaction between FeO_4^{2-} and OFX^- is very slow (Zheng et al. 2020; Han et al. 2018; Huang et al. 2017). On the other hand, the HCO_3^- will react with $OH^•$, thereby depleting free radicals in solution and reducing the reaction rate (Wang and Wang 2021).

However, the pH of the solution raised after bicarbonate hydrolysis is limited, and Fig. 4 also proves that the contribution of $OH^•$ is small. Therefore, HCO_3^- has only a small inhibitory effect on OFX degradation in the reaction system.

Fe^{3+} enhanced the OFX removal by Fe(VI) mostly via self-catalysis of Fe(VI) to generate more Fe(IV) or Fe(V) (Jiang et al. 2016; Ma et al. 2016; Zhao et al. 2018a). Moreover, NH_4^+ was reductive, which could promote the generation of Fe(IV) or Fe(V) from Fe(VI), thus improving the removal rate of OFX (Zhao et al. 2018b). Since HA and OFX compete with Fe(VI), HA has a significant inhibitory effect on the Fe(VI) degradation of OFX (Sharma et al. 2016; Horst et al. 2013).

Intermediate products and degradation pathways

Through a study of relevant references and Q-TOF LC/MS analysis of intermediate products of OFX degradation (Michael et al. 2013; Bi et al. 2019; Xue et al. 2017; Meng et al. 2021; Jin et al. 2021), and possible degradation pathways were proposed (Fig. 6). There are two main ways in which Fe(IV) degrades OFX. One of the degradation pathways is as follows: Firstly, the methyl group on the benzoxazine ring of OFX was carboxylated to form P1 (m/z = 391.1). P1 was then converted to P3 (m/z = 303.1) through decarboxylation. After the opening of the piperazine and oxazine rings, P3 was transformed into P5 (m/z = 178.1), and finally, P7 (m/z = 110.0) was formed through pyridine ring opening, defluorination, deamination, and hydroxylation. The other degradation pathway is as follows: OFX was converted into P2 (m/z = 337.1) through pyridine ring opening, and then P4 (m/z = 218.1) was formed by the opening of the piperazine and oxazine rings. P4 was finally transformed into P6 (m/z = 122.0) by deamination, defluorination, and dehydroxylation. P6 and P7 were further oxidized to form small molecular intermediates, which were finally decomposed into small molecular acids, CO_3^{2-}, H_2O, NO_3^-, and minerals (Zhou et al. 2021).

Conclusion

This study showed that Fe(VI) is an effective oxidant for the degradation of OFX. The degradation rate of OFX by Fe(VI) was in accordance with the second-order kinetic equation. OFX degradation by Fe(VI) was directly proportional to the initial concentration of Fe(VI) and temperature and inversely proportional to the pH. Under the conditions of [Fe(VI)]:[OFX] = 15:1, $T = 25$℃, and pH = 7.0, the removal efficiency of 8 μM OFX reached more than 90% in 4 min. Seven intermediates were identified by Q-TOF LC/MS, and the opening loop, decarboxylation, breaking the C-N bond, and deamination were the main reaction processes identified in their formation. In conclusion, Fe(VI) advanced

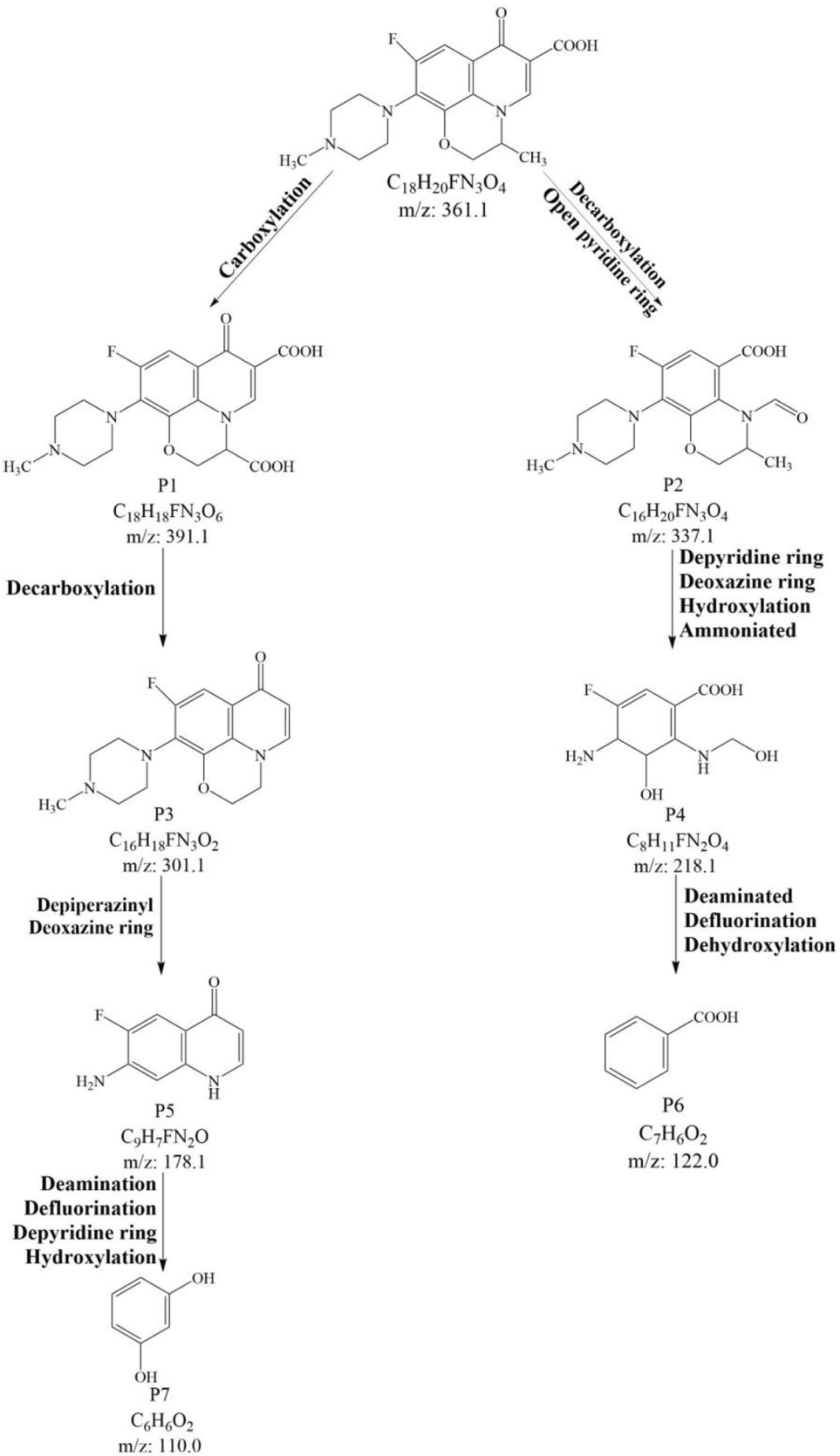

Fig. 6 Pathways of OFX degradation by Fe(VI)

oxidation technology has obvious advantages in the treatment of wastewater containing OFX.

Supplementary Information The online version contains supplementary material available at https://doi.org/10.1007/s11356-022-18949-x.

Acknowledgements We would like to thank the Faculty of Geosciences and Environmental Engineering of Southwest Jiaotong University for their help with the experimental analysis work.

Author contribution Yanghan Chen: investigation, resources, visualization, writing – original draft; Qiuye Jin: conceptualization, methodology, formal analysis, data curation, visualization; Zhaomin Tang: validation, supervision, writing – review and editing, funding acquisition, project administration.

Funding This work was supported by the National Natural Science Foundation of China (Grant No. 51803174).

Data availability All data generated or analyzed during this study are included in this published article and its supplementary information files.

Declarations

Ethics approval and consent to participate This manuscript does not report on or involve the use of any animal or human data or tissue.

Consent for publication This manuscript does not contain data from any individual person.

Competing interests The authors declare no competing interests.

References

Bi W, Jin Y, Wang H (2019) Migration and transformation of ofloxacin by free chlorine in water distribution system. Water 11(4):817

Cerqueira F, Matamoros V, Bayona J, Elsinga G, Hornstra LM, Pina B (2019) Distribution of antibiotic resistance genes in soils and crops. A field study in legume plants (*Vicia faba* L.) grown under different watering regimes. Environ Res 170:16–25

Chen P, Blaney L, Cagnetta G, Huang J, Wang B, Wang Y, Deng S, Yu G (2019) Degradation of ofloxacin by perylene diimide supramolecular nanofiber sunlight-driven photocatalysis. Environ Sci Technol 53(3):1564–1575

Chen X, Yao J, Xia B, Gao N, Zhang Z (2020) Influence of pH and DO on the ofloxacin degradation in water by UVA-LED/TiO2 nanotube arrays photocatalytic fuel cell: mechanism, ROSs contribution and power generation. J Hazard Mater 383(Feb.5):121220.1-121220.11

Elmolla ES, Chaudhuri M (2010) Degradation of amoxicillin, ampicillin and cloxacillin antibiotics in aqueous solution by the UV/ZnO photocatalytic process. J Hazard Mater 173:445–449

Gong S, Sun Y, Zheng K, Jiang G, Li L, Feng J (2020) Degradation of levofloxacin in aqueous solution by non-thermal plasma combined with Ag_3PO_4/activated carbon fibers: mechanism and degradation pathways. Sep Purif Technol 250:117264

Gorito AM, Ribeiro AR, Gomes CR, Almeida CMR, Silva AMT (2018) Constructed wetland microcosms for the removal of organic micropollutants from freshwater aquaculture effluents. Sci Total Environ 644:1171–1180

Han Q, Dong WY, Wang HJ, Liu TZ, Tian Y, Song X (2018) Degradation of tetrabromobisphenol A by ferrate(VI) oxidation: performance, inorganic and organic products, pathway and toxicity control. Chemosphere 198:92–102

Horst C, Sharma VK, Baum JC, Sohn M (2013) Organic matter source discrimination by humic acid characterization: synchronous scan fluorescence spectroscopy and Ferrate(VI). Chemosphere 90:2013–2019

Hu JY, Wang W, Zhu Z, Zhu Z, Chang H, Pan F, Lin BL (2007) Quantitative structure-activity relationship model for prediction of genotoxic potential for quinolone antibacterials. Environ Sci Technol 41:4806–4812

Huang JH, Wang YH, Liu GG, Chen P, Wang FL, Ma JS, Li FH, Liu HJ, Lv WY (2017) Oxidation of indometacin by ferrate(VI): kinetics, degradation pathways, and toxicity assessment. Environ Sci Pollut R 24:10786–10795

Huang YH, Liu Y, Du PP, Zeng LJ, Mo CH, Li YW, Lu HX, Cai QY (2019) Occurrence and distribution of antibiotics and antibiotic resistant genes in water and sediments of urban rivers with black-odor water in Guangzhou, South China. Sci Total Environ 670:170–180

Jara D, Bello-Toledo H, Domínguez M, Cigarroa C, Fernández P, Vergara L, Quezada-Aguiluz MA, Opazo- Capurro AF, Lima GA, González-Rocha G (2020) Antibiotic resistance in bacterial isolates from freshwater samples in Fildes Peninsula, King George Island. Antarctica Sci Rep 10(1):3145

Jia A, Wan Y, Xiao Y, Hu J (2012) Occurrence and fate of quinolone and fluoroquinolone antibiotics in a municipal sewage treatment plant. Water Res 46:387–394

Jiang C, Ji Y, Shi Y, Chen J, Cai T (2016) Sulfate radical-based oxidation of fluoroquinolone antibiotics: kinetics, mechanisms and effects of natural water matrices. Water Res 106:507–517

QY Jin, DY Ji, YH Chen, ZM Tang, YS Fu (2021) Kinetics and pathway of levofloxacin degradation by ferrate(VI) and reaction mechanism of catalytic degradation by copper sulfide. Sep Purif Technol 282

Li C, Li XZ, Graham N (2005) A study of the preparation and reactivity of potassium ferrate. Chemosphere 61:537–543

Liu X, Zhang H, Li L, Fu C, Tu C, Huang Y, Wu L, Tang J, Luo Y, Christie P (2016) Levels, distributions and sources of veterinary antibiotics in the sediments of the Bohai Sea in China and surrounding estuaries. Mar Pollut Bull 109:597–602

Liu HX, Chen J, Wu NN, Xu XX, Qi YM, Jiang LJ, Wang XH, Wang ZY (2019) Oxidative degradation of chlorpyrifos using ferrate(VI): kinetics and reaction mechanism. Ecotox Environ Safe 170:259–266

Luo Z, Li X, Zhai J (2015) Kinetic investigations of quinoline oxidation by ferrate(VI). Environ Technol 37(9–12):1–19

Ma L, Lam WWY ,Lo PK ,Lau KC, Lau TC (2016) Ca^{2+}-Induced Oxygen Generation by FeO_4^{2-} at pH 9–10. Angewandte Chemie 128(9): 3064-3068 10.1002/ange.201510156

Meng FQ, Wang YL, Chen Z, Hu J, Ma W (2021) Synthesis of CQDs@FeOOH nanoneedles with abundant active edges for efficient electro-catalytic degradation of levofloxacin: degradation mechanism and toxicity assessment. Appl Catal B- Environ 282:119597

Michael I, Hapeshi E, Acena J, Perez S, Petrovic M, Zapata A, Barceló D, Malato S, Fatta-Kassinos D (2013) Light-induced catalytic transformation of ofloxacin by solar Fenton in various water matrices at a pilot plant: mineralization and characterization of major intermediate products. Sci Total Environ 461:39–48

Noorhasan N, Patel B, Sharma VK (2010) Ferrate(VI) oxidation of glycine and glycylglycine: kinetics and products. Water Res 44:927–935

Peng H, Pan B, Wu M, Liu R, Zhang D, Wu D, Xing B (2012) Adsorption of ofloxacin on carbon nanotubes: solubility, pH and cosolvent effects. J Hazard Mater 211–212:342–348

Peterson JW, Gu B, Seymour MD (2015) Surface interactions and degradation of a fluoroquinolone antibiotic in the dark in aqueous TiO_2 suspensions. Science of the Total Environment 532(nov.1):398–403

Pi R, Liu H, Sun X, Zhang R, Zhang J, Sharma VK (2021) Strategy of periodic reverse current electrolysis to synthesize ferrate(VI): enhanced yield and removal of sulfachloropyridazine. Sep Purif Technol 263:118420

Radjenovic J, Petrovic M, Barceló D (2007) Analysis of pharmaceuticals in wastewater and removal using a membrane bioreactor. Anal Bioanal Chem 387(4):1365–1377

Sanganyado E, Gwenzi W (2019) Antibiotic resistance in drinking water systems: occurrence, removal, and human health risks. Sci Total Environ 669:785–797

Shao B, Dong H, Sun B, Guan X (2019). Role of ferrate(IV) and ferrate(V) in activating ferrate(VI) by calcium sulfite for enhanced oxidation of organic contaminants. Environ Sci Technol 53: 894-902 10.1021/acs.est.8b04990

Sharma VK, Chen L, Zboril R (2016) Review on high valent FeVI 279 (Ferrate): A sustainable green oxidant in organic chemistry and transformation of pharmaceuticals. ACS Sustain Chem Eng 4:18–34

Shin J, Gunten U, Reckhow D, Allard S, Lee Y (2018) Reactions of ferrate(VI) with iodide and hypoiodous acid: kinetics, pathways, and implications for the fate of iodine during water treatment. Environ Sci Technol 52:7458–7467

Tong X, Wang X, He X, Xu K, Mao F (2019) Effects of ofloxacin on nitrogen removal and microbial community structure in constructed wetland. Sci Total Environ 656:503–511

Van Boeckel TP, Pires J, Silvester R, Zhao C, Song J, Criscuolo NG, Gilbert M, Bonhoeffer S, Laxminarayan R (2019) Global trends in antimicrobial resistance in animals in low-and middle-income countries. Sci 365(6459):eaaw1944

Wang J, Chen H (2020) Catalytic ozonation for water and wastewater treatment: recent advances and perspective. Sci Total Environ 704(feb.20):135249.1-135249.17

Wang JL, Wang SZ (2018) Microbial degradation of sulfamethoxazole in the environment. Appl Microbiol Biotechnol 102:3573–3582

Wang JL, Wang SZ (2018) Activation of persulfate (PS) and peroxymonosulfate (PMS) and application for the degradation of emerging contaminants. Chem Eng J 334:1502–1507

Wang JL, Wang SZ (2019) Preparation, modification and environmental application of biochar: a review. J Clean Prod 227:1002–1022

Wang SZ, Wang JL (2019) Activation of peroxymonosulfate by sludge-derived biochar for the degradation of triclosan in water and wastewater. Chem Eng J 356:350–358

Wang JL, Wang SZ (2020) Reactive species in advanced oxidation processes: formation, identification and reaction A. Chem Eng J 401:126158

Wang JL, Wang SZ (2021) Effect of inorganic anions on the performance of advanced oxidation processes for degradation of organic contaminants. Chem Eng J 411(20):128392

Wang JL, Zhuan R (2020) Degradation of antibiotics by advanced oxidation processes: an overview. Sci Total Environ 701:135023

Wang Z, Jiang J, Pang S, Zhou Y, Cuan C, Gao Y, Li J, Yang Y, Qu W, Jiang C (2018) Is sulfate radical really generated from peroxydisulfate activated by iron(II) for environmental decontamination? Environ Sci Technol 52(19):11276–11284

Wang HY, Wang SJ, Jiang JQ, Shu J (2019) Removal of sulfadiazine by ferrate(VI) oxidation and montmorillonite adsorption-synergistic effect and degradation pathways. J Enviro Chem Eng 7:103225

Wang JL, Chu LB, Wojnárovits L, Takács E (2020) Occurrence and fate of antibiotics, antibiotic resistant genes (ARGs) and antibiotic resistant bacteria (ARB) in municipal wastewater treatment plant: an overview. Sci Total Environ 744:140997

Wang S, Shao B, Qiao J, Guan X (2020b) Application of Fe(VI) in abating contaminants in water: state of art and knowledge gaps. Front Env Sci Eng 15:80

Watanabe K, Numata-Watanabe K, Hayasaka S (2001) Methicillin-resistant staphylococci and ofloxacin-resistant bacteria from clinically healthy conjunctivas. Ophthalmic Res 33:136–139

Wilde ML, Mahmoud WMM, Kuemmerer K (2013) Oxidation-coagulation of beta-blockers by K_2FeVIO_4 in hospital wastewater: assessment of degradation products and biodegradability. Sci Total Environ 452–453:137–147

Xue H, Hu C, Peng J, Wang L, Wang Y, Ji N, Wen X (2017) Degradation of ofloxacin in aqueous solution with UV/H_2O_2. Desalin Water Treat 72(APR):386–393

Zajicek P, Kolar M, Prucek R, Ranc V, Bednar P, Varma RS, Sharma VK, Zboril R (2015) Oxidative degradation of triazine- and sulfonylurea-based herbicides using Fe(VI): the case study of atrazine and iodosulfuron with kinetics and degradation products. Sep Purif Technol 156:1041–1046

Zhang P, Zhang G, Dong J, Fan M, Zeng G (2012) Bisphenol A oxidative removal by ferrate (Fe(VI)) under a weak acidic condition. Sep Purif Technol 84:46–51

Zhang QQ, Ying GG, Pan CG, Liu YS, Zhao JL (2015) Comprehensive evaluation of antibiotics emission and fate in the river basins of China: source analysis, multimedia modeling, and linkage to bacterial resistance. Environ Sci Technol 49:6772–6782

Zhao S, Liu X, Cheng D, Liu G, Liang B, Cui B, Bai J (2016) Temporal-spatial variation and partitioning prediction of antibiotics in surface water and sediments from the intertidal zones of the Yellow River Delta, China. Sci Total Environ 569–570:1350–1358

Zheng Q, Wu NN, Qu RJ, Albasher G, Cao WM, Li BB, Alsultan N, Wang ZY (2020) Kinetics and reaction pathways for the transformation of 4-tert-butylphenol by ferrate(VI). J Hazard Mater 2020:123405

Zhou Y, Gao Y, Jiang J, Shen Y, Pang S, Song Y, Guo Q (2021) A comparison study of ofloxacin degradation by peroxymonosulfate and permanganate: kinetics, products and effect of quinone group. J Hazard Mater 403:123834

Zhao J, Wang Q, Fu Y, Peng B, Zhou G (2018a) Kinetics and mechanism of diclofenac removal using ferrate(VI): Roles of Fe^{3+}, Fe^{2+}, and Mn^{2+}. Environ Sci Pollut R 25: 22998-23008 10.1007/s11356-018-2375-6

Zhao J, Liu Y, Wang Q, Fu Y, Lu X, Bai XF (2018b) The self-catalysis of ferrate (VI) by its reactive byproducts or reductive substances for the degradation of diclofenac: kinetics, mechanism and transformation products. Sep Purif Technol 192: 412-418 10.1016/j.seppur.2017.10.030